



# Preparation, characterization and antioxidant activity of polysaccharides selenides from Qingzhuan Dark Tea

Hongfu ZHOU<sup>1#</sup>, Shiyue WANG<sup>1#</sup>, Ziyao WANG<sup>1</sup>, Wenjing XIE<sup>1</sup>, Cai WANG<sup>1\*</sup>, Min ZHENG<sup>1\*</sup> 

## Abstract

The effective selenylated polysaccharides (refer as TPS-Se) with an average molecular weight ( $M_w$ ) of  $3.109 \times 10^4$  Da was synthesized by the reduction of sodium selenite with ascorbic acid in the presence of Qingzhuan Dark Tea polysaccharides (TPS). The selenium (Se) content of TPS-Se was up to 37.05%. The differences between TPS and TPS-Se were compared in morphology, structure, antioxidant activity, and molecular weight using FT-IR, Raman spectroscopy, X-ray diffraction (XRD), and X-ray photoelectron spectroscopy (XPS), SEM, AFM, and Integrated thermal gravimetric analysis. The results indicated that  $Se^{4+}$  was reduced to  $Se^0$  by ascorbic acid. Further, the  $Se^0$  atoms aggregate into Se nuclei and bind to the C=O from TPS. Also, TPS-Se exhibited higher DPPH and ABTS radical-scavenging abilities than TPS. This difference may be attributed to the fact that Se has good antioxidant activity. The test results demonstrated that TPS-Se was prepared successfully by reducing sodium selenite with ascorbic acid, which exhibited a higher radical-scavenging ability. Finally,  $LD_{50}$  value of 136.89 mg/kg, with a 95% confidence interval of 102.82~182.82 mg/kg, was determined by gavage administration for TPS-Se's.

**Keywords:** Qingzhuan Dark Tea polysaccharides; selenium; characterization; antioxidant activity; acute toxicity.

**Pratica Application:** Develop Qingzhuan Dark Tea for pharmaceutical industry.

## 1 Introduction

Free radicals in the human body can cause oxidation and damage the cells, leading to aging and various diseases. The concentration of free radicals in the human body increases with age, and the ability to clear reduces (Cai et al., 2018). At the same time, endogenous antioxidants are restricted by content, spatial location, and scavenging energy. Therefore, timely intake of exogenous antioxidants is essential for maintaining the body's oxygen balance (Bai & Bai, 2021). Common antioxidants include natural and synthetic antioxidants, where synthetic antioxidants have a good antioxidant effect but exhibit certain toxicity and side effects on the body. On the other hand, the natural antioxidant is safe, stable, and has high antioxidant activity, but has drawbacks include low content, difficulty obtaining, and high price (Souad et al., 2021).

Natural polysaccharides are elements revealing antioxidant activity. They exhibit advantages such as being non-toxic and having good biocompatibility compared with drugs by chemical synthesis (Huang et al., 2017). Polysaccharides increase the antioxidant enzyme activity, scavenging free radicals, inhibiting lipid peroxidation, protecting biofilm, antioxidation, and anti-aging. However, studies on polysaccharides' antioxidant activity and mechanism are still at an exploratory stage (Liu et al., 2018) (Mei et al., 2017).

With increasing attention paid to the benefits for Qingzhuan Dark Tea's human bodies, such as reducing weight and fat (Monobe et al., 2008), antioxidant ability (Xia, 2019), improvement

of intestinal function (Li, 2018), and bacteriostatic effect (Mao, 2019). One of the main components of Qingzhuan Dark Tea is Polysaccharides, which is also one of the main components that play its physiological role (Ting et al., 2019). At present-day, lots of studies have verified that polysaccharides from Qingzhuan Dark Tea have the antioxidant ability and competitive inhibition of  $\alpha$ -glycosidase activity (Ting et al., 2019). However, there are few studies on polysaccharides of Qingzhuan Dark Tea; further studies about Qingzhuan Dark Tea are still needed.

Selenium imparts a wide range of biological functions in human and animal health (Rayman, 2000) as an essential trace mineral. Extensive clinical and epidemiological studies were used to prove the health features of selenium and the relationship between the absence of selenium and various diseases. Selenium is part of the active site of many enzymes, such as glutathione peroxidase (GSH-Px) in cells, directly or indirectly affecting scavenging intracellular free radicals. However, inorganic selenium has strong toxicity that is harmful to the human body and difficult to use (Letavayová et al., 2006) (Li et al., 2008).

In this research, polysaccharides of Qingzhuan Dark Tea bind to selenium to form a polysaccharides selenide complex (refer as TPS-Se). A series of characterizations were carried out to determine the chemical structure and its antioxidant activity. The conversion of inorganic selenium to organic selenium combined the biological activity of polysaccharides and selenium, and hence greatly reduced the toxicity of selenium and formed

Received 16 Oct., 2021

Accepted 12 Dec., 2021

<sup>1</sup>Xianning Medical College, Hubei University of Science and Technology, Xianning, Hubei, China

\*Corresponding author: [xyzhengmin@hbust.edu.cn](mailto:xyzhengmin@hbust.edu.cn)

<sup>#</sup>These authors have contributed equally to this work and both are co-first authors.

a good selenium supplement. We categorized its structure and morphology and then compared the antioxidant activity of polysaccharides and TPS-Se, which provided a good basis for the follow-up pharmacological research.

## 2 Materials and methods

### 2.1 Materials

McLean reagents website is used to procure Qingzhuan Dark Tea (Hubei chibi Zhao Liqiao tea industry co., LTD.), HCl (national medicine group chemical reagent co., LTD.), ascorbic acid (analysis of pure, national medicine group chemical reagent co., LTD.),  $\text{Na}_2\text{SeO}_3$  (purity 99%, bought in Hubei xin embellish DE chemical co., LTD.), anhydrous ethanol, petroleum ether, and NaOH (analysis of pure). Other reagents used were of analytical grade, and the water used in all experiments was Milli-Q water.

### 2.2 Preparation polysaccharides selenides form Qingzhuan Dark Tea

The Qingzhuan Dark Tea powder (through 80 mesh sieve) was accurately weighed at 20.0 g. The petroleum ether was added as per the solid-liquid ratio of 1:10, the pigment was cleaned by heating at 60 °C for 3 h, and the tea residue was dried at 60 °C to a constant weight (Luo et al., 2012). Then 80% ethanol solution in the solid-liquid ratio of 1:10 was added to the tea residue, heated at 80 °C for 2 h to remove small molecules, and dried at 80 °C to a constant weight. The tea residue was added with ultra-pure water according to the solid-liquid ratio of 1:16 and extracted with water at 60 °C for 4 h. Then concentrate the water extract to 20 mL, add 60 mL anhydrous ethanol, and store at 4 °C for 12 h. The rough polysaccharides of Qingzhuan Dark Tea were obtained by freeze-drying (Ke et al., 2021). 1.0 g of Qingzhuan Dark Tea's rough polysaccharides were prepared into a 10 mg/mL polysaccharides solution. A polyamide column cleaned out

proteins and pigments. The eluent was collected, concentrated, and dialyzed for 48 h and then freeze-dried to obtain the refined polysaccharides of Qingzhuan Dark Tea (Yu, 2019).

Polysaccharides of Qingzhuan Dark Tea selenide are prepared by reducing sodium selenite with ascorbic (Ru et al., 2020). 90 mg TPS was added to 90 mL ultrapure water and stirred until fully dissolved at room temperature. Add 30 mL of 0.05 M  $\text{Na}_2\text{SeO}_3$  solution into TPS solution and stir for 1 min. Add 30 mL of 0.1M  $\text{V}_c$  solution and stir for 12 h at room temperature (25 °C). After the reaction was completed, the obtained solution was dialyzed for 48 h, concentrated, and freeze-dried to obtain polysaccharides selenium (TPS-Se) of Qingzhuan Dark Tea. The specific process is shown in Figure 1.

### 2.3 Characterization

The graphite furnace atomic absorption spectrometry and ContraA 700 atomic absorption spectrometer techniques were used to determine the selenium content in TPS-Se.

10 mg TPS, TPS-Se, and KBr powders were weighed and pressed into sheets, respectively. The Fourier transform infrared spectroscopy was used to measure the infrared spectra of TPS and TPS-Se in the range of 4000~400  $\text{cm}^{-1}$  (Zheng et al., 2020).

The TPS and TPS-Se were dissolved in distilled water, then placed on the microscope slide and fixed on the Raman spectral detector (Invia Reflex, England, Laser 532 nm, displacement range of 3000~100  $\text{cm}^{-1}$ ). Control IV (WITEC) acquisition software is used for Raman imaging setup.

TPS, TPS-Se, and  $\text{NaSe}_2\text{O}_3$  were ground into powder, and the EMPYREAN X-ray diffractometer was used to determine the routine X-ray powder diffraction.

TPS, TPS-Se, and potassium selenate were ground into a powder. The surface elemental composition and binding



Figure 1. Flow chart of TPS-Se preparation.

valence of the samples were determined by Escalab 250XI X-ray photoelectron spectroscopy.

The HPGPC (High-Performance Gel Filtration Chromatography) method was used to determine the molecular weight and homogeneity of TPS and TPS-Se. 2 mg of TPS and TPS-Se were precisely weighed and dissolved in 400 L of 0.1 mol Na<sub>2</sub>NO<sub>3</sub> solution. The Waters 1525 HPLC and Ultrahydrogel™ Linear 300 mm×7.8 mm ID ×2 column with 2410 differential refractive detector emPower workstation determined TPS and TPS-Se uniformity and molecular weight distribution. The mobile phase was 0.1 mol/L Na<sub>2</sub>NO<sub>3</sub> solution, the flow rate was 0.9 mL/min, and the column temperature was 45 °C.

The TPS and TPS-Se were ground into powder and placed on conductive carbon tape. With the use of field emission scanning electron microscopy, the morphology of TPS and TPS-Se was observed.

TPS solution (10 µg/mL) and TPS-Se solution (10 µg/mL) were deposited on mica and then tested under an atomic force microscope.

A sample of 15 mg was collected and put into a STA449F3 synchronous thermal analyzer. The temperature was set at 10 °C/min in N<sub>2</sub> atmosphere, and the data from room temperature was recorded at 800 °C to analyze the thermal stability of the sample.

#### 2.4 Effects on antioxidant activities

The Zeynep Bakkaloglu (Bakkaloglu et al., 2021) and Sze-Yuen Lew's (Lew et al., 2020) method with slight modifications was used to measure the scavenging activity of TPS and TPS-Se DPPH radicals. Briefly, 2 mL of the solution at different concentrations (0.25~1.25 mg/mL) was mixed with 2 mL of 0.1 mmol/L DPPH ethanol solution. The mixture was shaken vigorously and incubated for 30 min at 25 °C in the dark. Finally, the absorbance was recorded at 517 nm on a microplate reader. The following Formula 1 calculated the DPPH radical inhibition (%):

$$\text{DPPH radical scavenging ability (\%)} = \left[ 1 - \frac{(A_a - A_b)}{A_c} \right] \times 100 \quad (1)$$

where A<sub>a</sub> refers to the sample mixed with DPPH solution, A<sub>b</sub> refers to the sample without DPPH solution, and A<sub>c</sub> is the absorbance of DPPH solution without the sample as a blank control.

The scavenging activity of TPS and TPS-Se against ABTS radical cation was measured by Arzu Kaska et al. (Kaska et al., 2021) and Iana Maria Cristino Pereira et al. (Pereira et al., 2020) with some modifications. Usually, 7.4 mmol/L of ABTS solution was reacted with 2.6 mmol/L of potassium persulfate to obtain ABTS radical cation (ABTS<sup>+</sup>). The mixture was kept in the dark for 12~16 h at room temperature, and the ABTS<sup>+</sup> solution was diluted to a stable absorbance of 0.70 ± 0.01 at 734 nm. Next, 1.4 mL of the sample at various concentrations (0.33~1.67 mg/mL) was mixed with 0.7 mL of the diluted ABTS<sup>+</sup> solution. The absorbance was measured at 734 nm using a microplate reader after the reaction at room temperature for 6 min. The following Formula 2 calculated the ability of TPS and TPS-Se to scavenge ABTS<sup>+</sup>:

$$\text{ABTS}^+ \text{ scavenging ability (\%)} = \left[ 1 - \frac{(A_1 - A_2)}{A_0} \right] \times 100 \quad (2)$$

where A<sub>1</sub> denotes the sample mixed with ABTS<sup>+</sup> solution, A<sub>2</sub> denotes sample without ABTS<sup>+</sup> solution, and A<sub>0</sub> is the absorbance of ABTS<sup>+</sup> solution without the sample as a blank control.

#### 2.5 Acute oral toxicity study

Sixty SPF C57BL/6 mice, male and female, weighing 18~25 g, were fed for one week under the conditions of room temperature 23 ± 2 °C, humidity 60%~70%, and free access to food and water. After 12 h of fasting, they were used for acute toxicity tests. Using the modified Kohl's method (Qing, 2013), the LD<sub>50</sub> of TPS and TPS-Se was detected by gavage, but the preliminary test could not determine the death dose of TPS, so the acute toxicity of TPS was seen by the maximum tolerated dose method. The minimum and maximum death doses of TPS-Se were 50 mg/kg and 245 mg/kg, respectively. After fasting for 12 h, 8 mice (female and male) were randomly selected for acute toxicity test of TPS. Eight mice were given 2000 mg/kg, 0.2 mL/10 g of TPS-Se orally at one time, and the other 8 mice were given the same volume of distilled water for continuous observation for 14 days. The poisoning symptoms and death of the mice were recorded.

Meanwhile, for the acute toxicity test of TPS-Se, another 40 (half female and half male) were selected. According to the dose of the preliminary examination, the ratio of formal experimental groups could be determined (Formula 3):

$$r = n \sqrt{d_k / d_i} \quad (3)$$

Where n denotes the number of formal experimental groups, n = 5 in this experiment, d<sub>i</sub> signifies the minimum death dose, d<sub>k</sub> refers to the maximum death dose, so the inter-group ratio r = 1.488.

The inter-group ratio was 1.488, which was divided into 5 dose groups such as 50 mg/kg, 75 mg/kg, 110 mg/kg, 165 mg/kg, and 245 mg/kg, respectively, with 8 females and males in each group given orally at one time. The activity of the mice was seen for 1 h after exposure, and close observation was required multiple times on the same day (especially within 4 h after exposure). After that, the mice were studied every day for 14 consecutive days. The feeding activity, urine and feces, mental and other systemic reactions, and death of the mice were recorded.

#### 2.6 Statistical analysis

The main experiments were performed and repeated at least three times unless stated otherwise. The experimental results were presented as the mean ± SD (standard deviation).

### 3 Results and discussion

#### 3.1 Selenylation modification of TPS Construction and morphology of SeNPs

To prepare TPS-Se, Na<sub>2</sub>SeO<sub>3</sub> was added to TPS aqueous solution and was fully mixed. Then Vc was added to convert

$\text{Se}_2\text{O}_3^{2-}$  into selenium atoms. Further, selenium atoms bind to TPS to generate the TPS-Se. The assembly process of TPS-Se can be noticed by monitoring the color change from colorless to light yellow or deep red, indicating the successful preparation of TPS-Se.

In Figure 2, the principle of selenide polysaccharides preparation of Qingzhuan Dark Tea by sodium ascorbate selenite method is shown.

Figure 2 displays the reaction principle of polysaccharide selenides of Qingzhuan Dark Tea. At the outset, sodium selenite and polysaccharide were linked together. The sodium selenite on the polysaccharide was reduced to selenium atoms after adding Vc, and selenium was linked with polysaccharide in a simple substance-like manner to form the Qingzhuan Dark Tea polysaccharide selenide.

### 3.2 Molecular weight and determination of selenium content

By studying the data from Table 1, the Mn of TPS, TPS-Se was 8608 and 9349, and the Mn of TPS-Se increased by 741, which combined with selenium. The Mw of TPS was 30111, and TPS-Se was 31090. The Mw of TPS increased by 979, which combined with Se. The results showed that selenium had been mixed with polysaccharides successfully by the reaction of polysaccharides with sodium selenite-VC. The PDI index reduced from 3.50 to

**Table 1.** Molecular weight and Determination of selenium content.

	TPS	TPS-Se
$M_n$	8608	9349
$M_w$	30111	31090
PDI	3.50	3.32
Se (%)	-	37.05

TPS: Qingzhuan Dark Tea polysaccharides. TPS-Se: selenylated Qingzhuan Dark Tea polysaccharides.  $M_n$ : number-average molar mass of polysaccharides and selenylated polysaccharides.  $M_w$ : weight-average molecular weight of polysaccharides and selenylated polysaccharides. PDI: coefficient of dispersion of polysaccharides and selenylated polysaccharides. Se(%):Selenium content in selenylated polysaccharides.

3.32, stating that the molecular weight distribution of TPS-Se was more concentrated than that of TPS. The selenium content of TPS-Se was measured to be 37.05%, and it showed a large amount of selenium binds to TPS.

### 3.3 FT-IR and Raman analysis

The FT-IR spectra examining the characteristics of TPS-Se and native TPS are shown in Figure 3A. After combination with selenium, the main distinctive peaks of TPS-Se were the same as those of TPS, indicating that the basic skeleton did not change. The FT-IR spectra showed that the distinct rise of O-H appeared at  $3374\text{ cm}^{-1}$ , the typical peak of C-H appeared at  $2934\text{ cm}^{-1}$ , and the characteristic peak of C=O appeared at  $1608\text{ cm}^{-1}$  distinctive peak of TPS-Se at  $834\text{ cm}^{-1}$  was C-O-Se. These spectral features indicated that Se occurred in the polysaccharides. The absorption peak of O-H in TPS-Se becomes wider, indicating that the O-H bond decreases. The C=O absorption peak becomes longer and sharper than the C=O bond increase, and the absorption peak of C-O-Se also appears. Based on these results, it can be inferred that H in -CHO was replaced by selenium in the polysaccharide, forming a C-O-Se bond. Being rich in hydroxyl and carboxyl groups, TPS may expose many negative charges on the macro molecule's surface, which provided many binding sites for the reduced Se atoms leading to the growth of polysaccharides selenide.

The Raman spectrum is a vibration spectrum, which can complement the infrared range to provide complete and accurate information about molecular vibration state and molecular structure. Figure 3B shows the Raman spectra of TPS and TPS-Se. In the TPS-Se Raman spectrum, the peak at  $255.59\text{ cm}^{-1}$  corresponds to a marker band of selenium, confirming that selenium had bound to polysaccharides. These characteristic absorption peaks indicated that TPS-Se was effectively modified in selenylation.

### 3.4 XRD and XPS analysis

A method to determine the crystal shape and phase composition is via X-ray single-crystal diffraction (XRD). XRD experiments

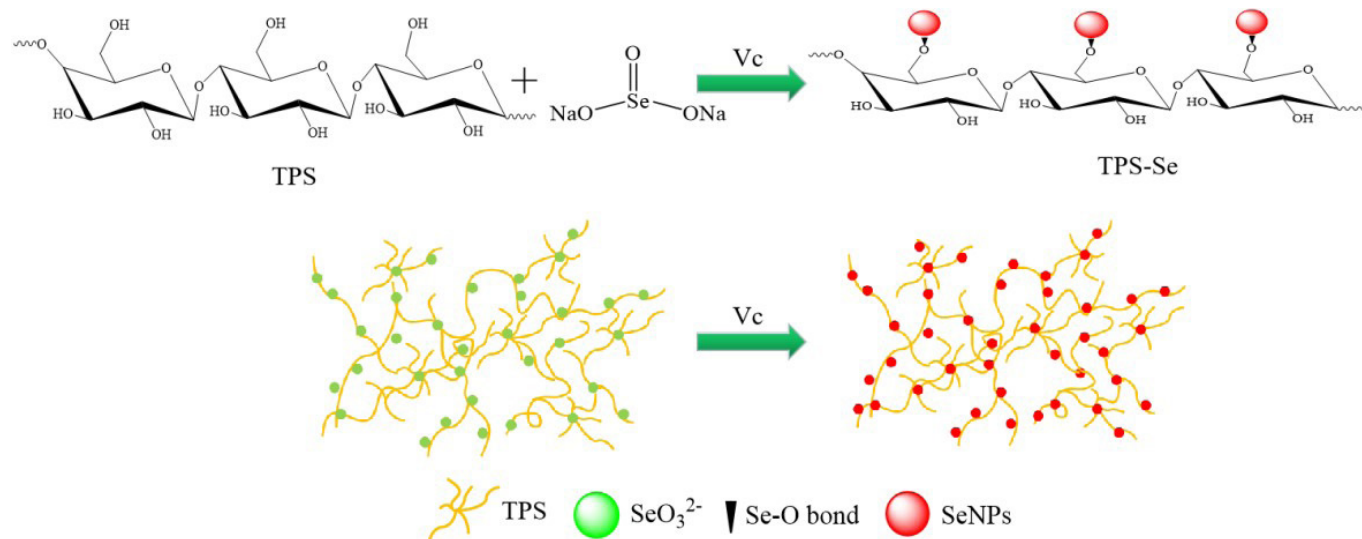


**Figure 2.** The reaction schematic of TPS-Se.

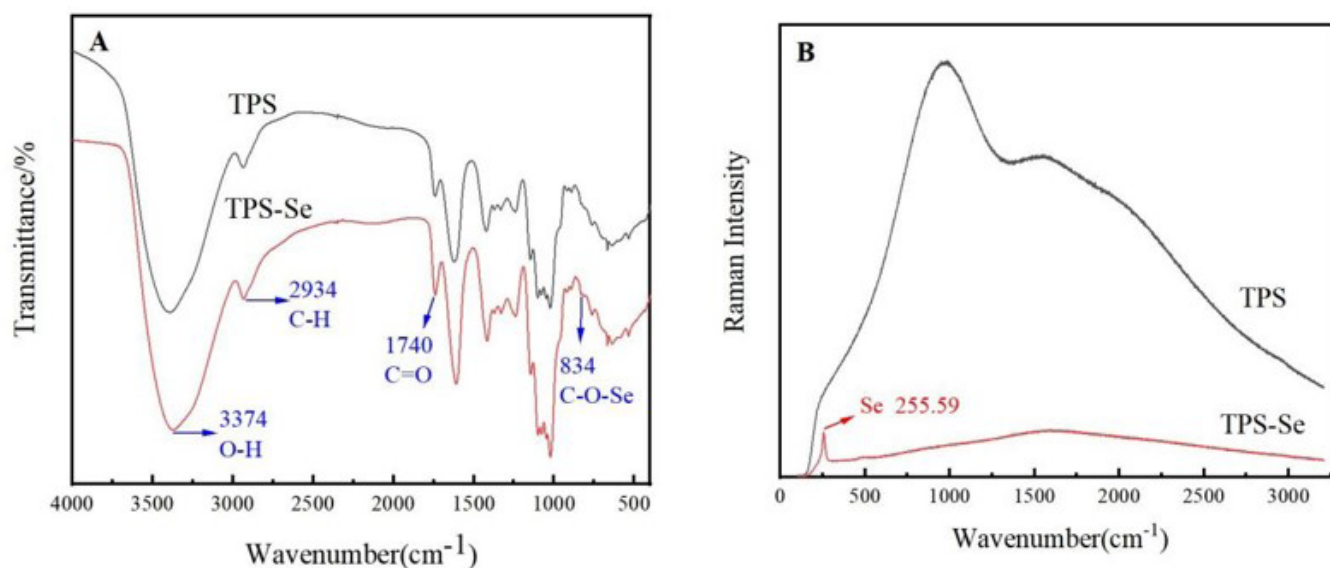


**Figure 3.** A: FT-IR spectra of TPS and TPS-Se, B: Raman scope of TPS and TPS-Se.

could evaluate the crystallinity of the TPS-Se; Figure 4 shows the XRD spectrum of TPS-Se with trigonal Se and TPS used for comparison. The trigonal-structured Se had two strong and sharp reflection peaks at  $2\theta$  of 24°, 31° and 50°, signifying the presence of the Se. However, the TPS-Se exhibited a broad reflection peak similar to that of TPS, and the three typical sharp peaks entirely disappeared in the TPS-Se systems. This result established that the Se in the TPS-Se matrix did not transform into a crystalline phase but continued in an amorphous state, leading to the disappearance of trigonal-structured selenium's strong and sharp reflection peaks. In Figure 4, there was no linear peak in the XRD patterns of TPS and TPS-Se, indicating that both TPS and TPS-Se were amorphous substances. In combination with the XRD standard card analysis of selenium essential elements, while retaining the characteristic peak of TPS, a new large envelope peak between 25~30 and 50~55 appeared. They corresponded to the distinct rise of selenium essential elements, indicating that the phase composition of TPS-Se was TPS and selenium essential elements. It was further revealed that selenium could bind to TPS in its elemental state.

XPS measurement was used to provide qualitative information of different surface elements on samples. XPS results of TSP and TSP-Se are shown in Figure 5. It can be concluded that TPS-Se retains the characteristic peak of TPS, and the 3D distinct rise of selenium appears at the binding energy of 56eV, indicating the presence of selenium in TPS-Se according to the full spectrum of TPS and TPS-Se in Figure 5A. The signal of TSP-Se (54 eV) was lower than that of K<sub>2</sub>SeO<sub>4</sub>, signifying that Se 3d signal was Se<sup>0</sup> and Se existed in the form of atoms (Figure 5B). The C 1s spectra of TSP and TSP-Se are shown in Figure 5C and Figure 5D. C 1s spectra of TSP were fitted with three components at 284.8, 285.5, and 286.8 eV, equivalent to photo-emission of C<sub>1</sub>en C-OH, and C=O, respectively. The signal intensity of C=O increases, and the intensity peak of C-OH decreases, as shown in Figure 5D. Combined with the changes of C=O bond and O-H bond in infrared, it can be inferred that in the

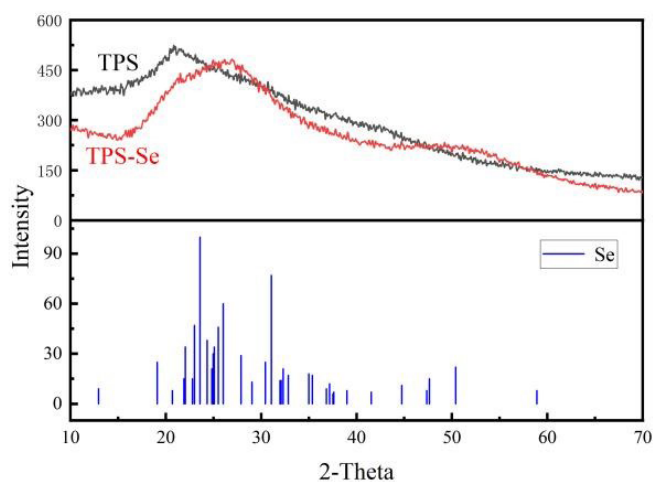


**Figure 4.** XRD image of TPS and TPS-Se.

reaction system of polysaccharide, sodium selenite, and Vc, part of the O-H bond is oxidized to the C=O double bond, where-H in-CHO is replaced by selenium; thus, promoting the reaction and generating TPS-Se.

### 3.5 SEM analysis

SEM is an important technique used to examine the surface morphology of polymers, including polysaccharides. Within the SEM image in Figure 6, the surface of TPS showed a rough concave shape, and the whole was relatively smoother than TPS-Se. The texture of TPS-Se is coarser than that of TPS, and spherical particles can be seen at high magnification, which is because of the gathering of selenium atoms in TPS. It indicated that sodium selenite is decreased to selenium atoms substance under the action of VC, and selenium atoms substance binds with TPS and aggregates on the surface of TPS.

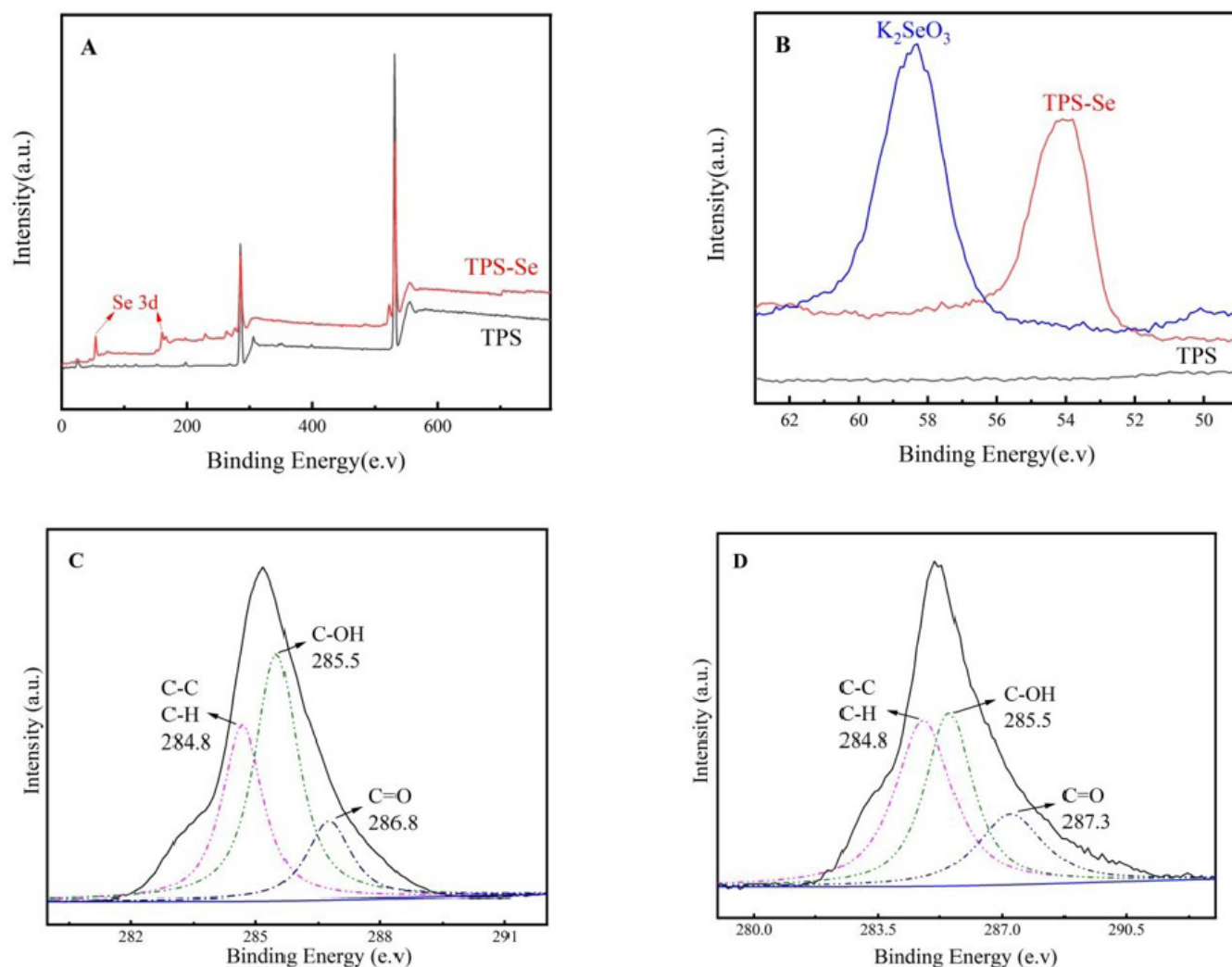


**Figure 5.** A: XPS spectra of TPS and TPS-Se; B: Se 3d spectra of TPS, TPS and  $\text{Na}_2\text{SeO}_3$ ; C: curve-fitting of C 1s spectra of TSP; D: curve-fitting of C 1s spectra of TPS-Se.

### 3.6 AFM analysis

AFM provides direct visualization of morphological features, molecule motion, linear chains, aggregates, helices, etc. Planar and 3D AFM images of TPS and TPS-Se are shown in Figure 7. As shown in Figure 7, TPS-Se exhibited a smooth surface morphology with a lot of hilly aggregates. The height of hilly aggregates was distributed from 0 to 18 nm. At the same time, TPS presented a conical lump characteristic of surface morphology, and the conical lump's average size was distributed in the range of 0~14 nm. The accumulation of TPS-Se was much more than that of TPS, suggesting that the aggregation effect had occurred and was more serious than that of TPS. These results indicated that the aggregation effect had increased due to the introduction of selenium, which enhanced the conformation, molecular weight, and even bioactivity.

### 3.7 Integrated thermal gravimetric analysis

Figure 8 shows a heat loss curve (TG) and a heat loss rate curve (DTG) of TPS and TPS-Se at the program heating rate

of 10 °C/min. After studying the trends of these two curves, they reveal the distribution of the pyrolysis products between the gas-solid phases. The sample pyrolysis process can be divided into four parts: Part 1 is the water loss process, where the TG curve has a slight and gentle decrease, and the DTG line reflects the small heat loss rate; the Part 2 is the sample preheating process, which has a slow reaction of the internal tissue, and small amounts of volatile gas escapes after the DTG curve began to change; Part 3 is the main pyrolysis process, where both curves drop sharply, the sample undergoes severe pyrolysis process, possibly accompanied by combustion. Part 4 is a slow decomposition process of residues, mainly for the matter that is not suitable for pyrolysis, and which produces residues such as ash. As per the TG image of TPS and TPS-Se, the weightlessness at 100~150 °C is due to the evaporation of water. The amount of water in TPS is higher than that in TPS-Se, as depicted in Figure 8A. The weightlessness between 200~350 °C is due to the combustion weightlessness of organic matter. TPS gradually becomes flat after 350 °C, while TPS-Se gradually becomes flat after 450 °C, as seen from Figure 8A. In

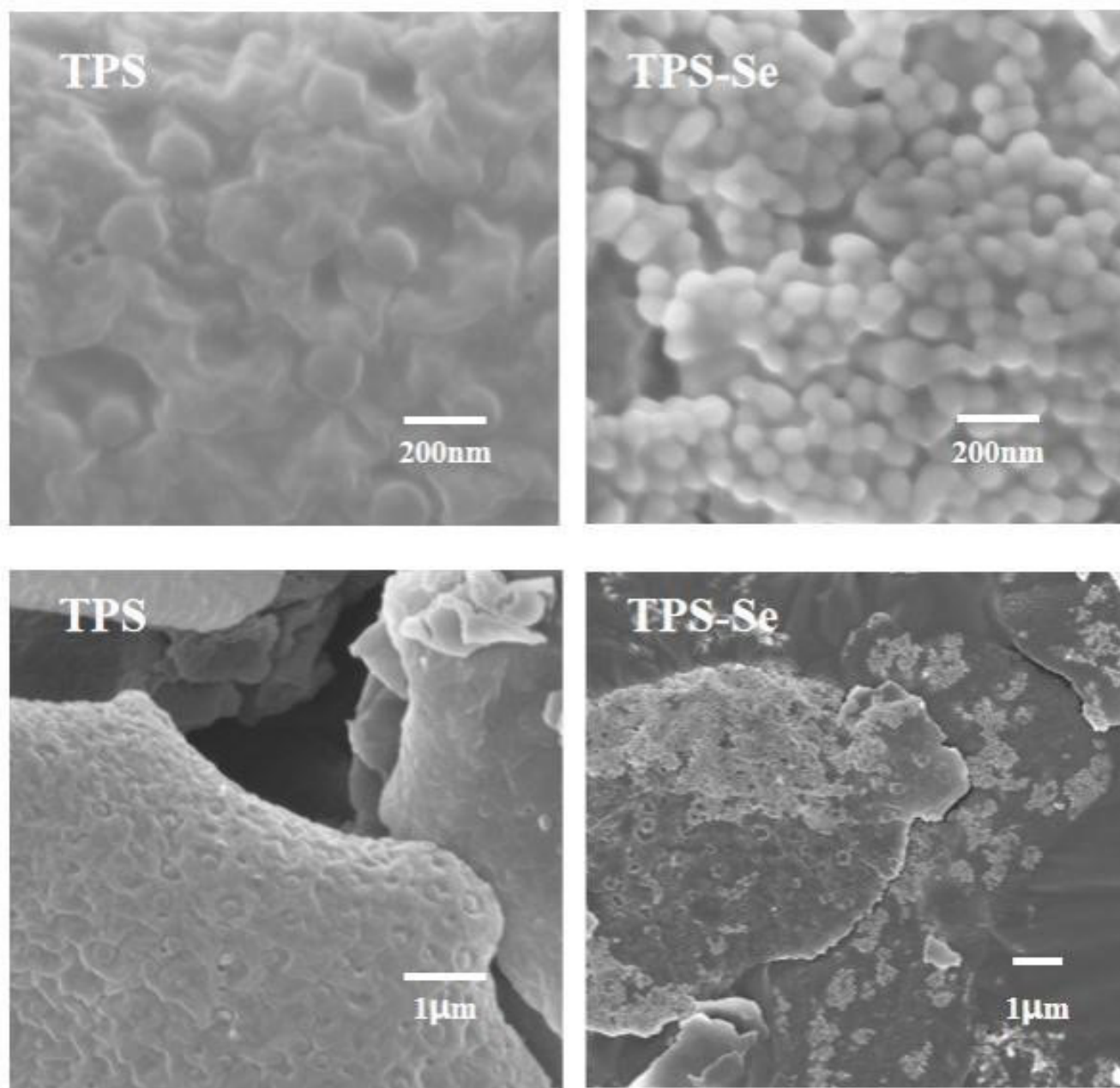


**Figure 6.** SEM images of TPS and TPS-Se.

Figure 8B, TPS-Se appears a downward endothermic peak at 370.5° C. It shows that the combustion of selenium causes the endothermic peak at 370.5 °C, and the weight loss of TPS-Se is more than that of TPS in Figure 8A, which further indicates that selenium combines with TPS.

### 3.8 DPPH radical-scavenging activities of TPS and TPS-Se

DPPH radical has been efficiently utilized to assess the free-radical scavenging activity of antioxidants. Figure 9 depicts the scavenging abilities of the TPS and TPS-Se against the DPPH radicals. At the concentrations of 0~1.0 mg/mL, all

the TPS and TPS-Se exhibited scavenging activities against DPPH radicals in a concentration-dependent manner. We can observe that the scavenging activity of TPS-Se is advanced than TPS at all concentrations, indicating that selenylation enhanced the inhibitory effect. Previous studies have shown that notable scavenging activities emerged in polysaccharides with selenylation. Therefore, there were two factors responsible for such enhancement on scavenging activity: selenium could interrupt the radical chain reactions to reinforce the antioxidant activity, and the TPS-Se with the large specific surface area could provide a lot of active sites to react with free radicals and suppress the reactions between the free radicals.

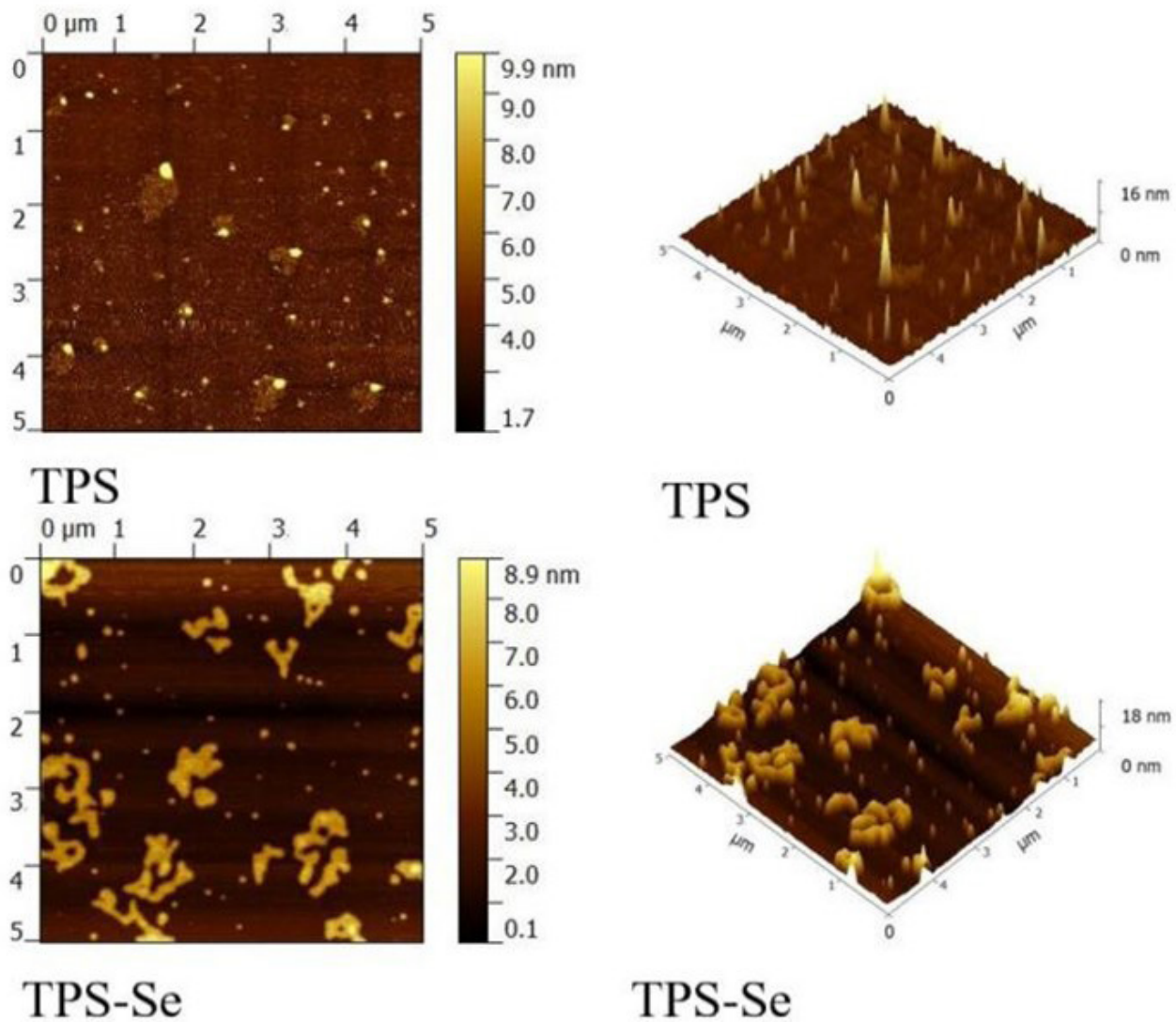


Figure 7. AFM images of TPS and TPS-Se.

### 3.9 ABTS radical-scavenging activities of TPS and TPS-Se

The ABTS radical cation ( $ABTS^+$ ) was commonly used to evaluate the total antioxidant activity of a single compound and complex mixtures. Figure 10 depicts the inhibitory effect of TPS and TPS-Se on  $ABTS^+$ . At the concentrations of 0.0~1.0 mg/mL, almost all the scavenging activities increased in a dose-dependent manner. We can observe that the scavenging activity of TPS-Se is higher than TPS at all concentrations, indicating that selenylation had a positive effect on the antioxidant activity. The two factors responsible for such enhancement on scavenging activity are: selenium could interrupt the radical chain reactions to reinforce the antioxidant activity, and the TPS-Se with the large specific surface area could provide many active sites to react with free radicals and could provide the reactions between the free radicals.

### 3.10 Acute oral toxicity study

**TPS group:** the experimental results were studied for 14 days consecutively. No deaths among mice were found, no abnormal reactions such as restlessness after administration, no increase in the secretion, and clean fur were seen. The TPS group showed no strange behavior compared with normal saline. TPS can be considered a non-toxic natural extract.

**TPS-Se group:** after 1 h of intragastric administration, the mice displayed lethargy, immobility, decreased activity, low diet, and water, and then began to die 6 h later. The experimental results are shown in Table 2:

Since the mortality rate of the maximum dose group was less than 100% but more than 70%,  $LD_{50}$  was calculated by the

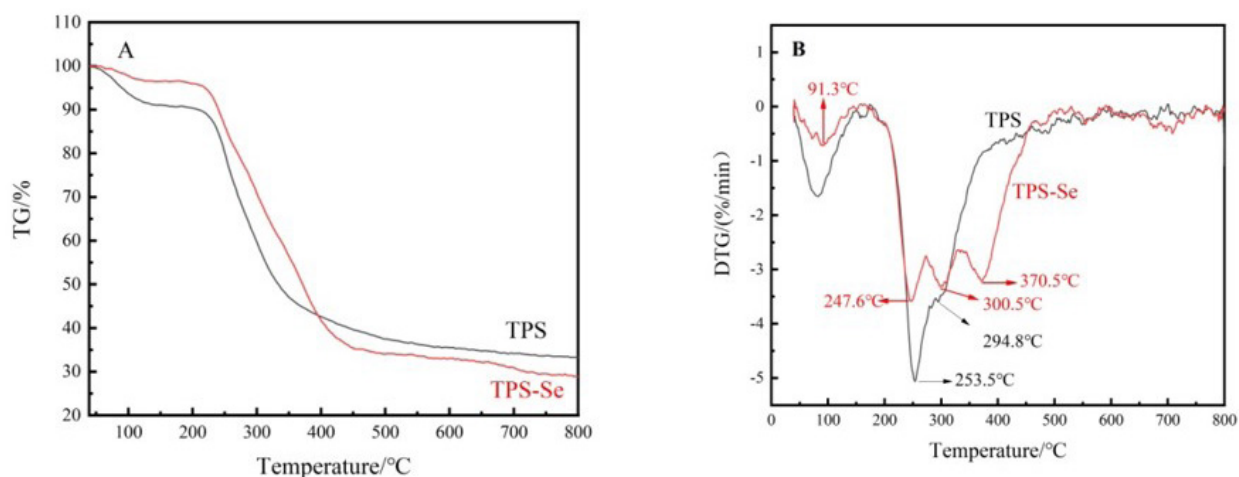


Figure 8. A: TG image of TPS and TPS-Se; B: DTG image of TPS and TPS-Se.

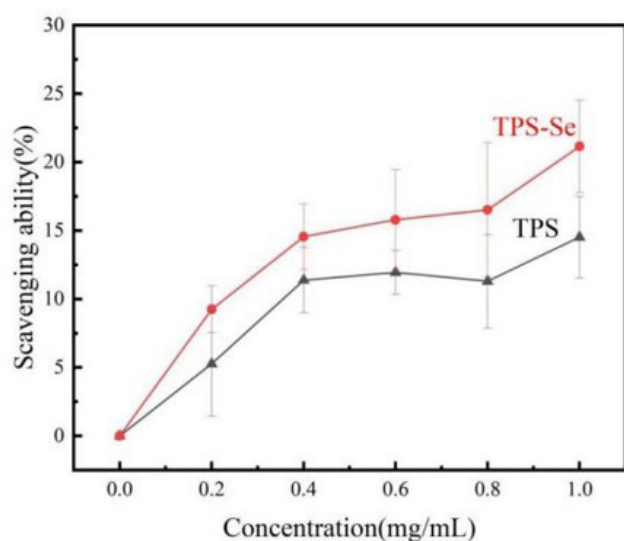


Figure 9. TPS and TPS-Se DPPH radical-scavenging activities.

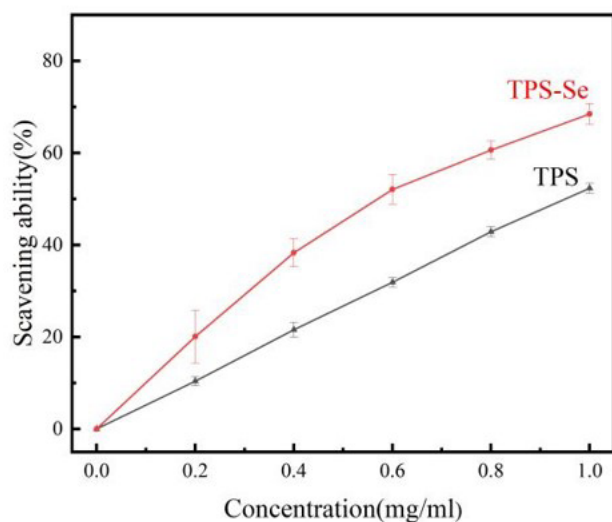


Figure 10. TPS and TPS-Se ABTS radical-scavenging activities.

Table 2 TPS-Se LD<sub>50</sub> official experimental results

dose(mg/kg)	50	75	115	165	245
P(%)					
TPS-Se	0	12.5	37.5	62.5	87.5

TPS-Se: selenylated Qingzhuang Dark Tea polysaccharides. P(%): daeth rate of mice.

revised formula. LD<sub>50</sub> = 136.89 mg/kg, with 95% confidence interval of 102.82~182.82 mg/kg.

TPS is selenized to obtain TPS-Se, which is converted from the inorganic Selenium form of Na<sub>2</sub>SeO<sub>3</sub> to the organic form of TPS-Se. Currently, it has been reported that the LD<sub>50</sub> of Na<sub>2</sub>SeO<sub>3</sub> is 11.75 mg/kg for Wistar rats and 3.86 mg/kg for Kunming mice. The experimental results of this study displayed that The LD<sub>50</sub> of TPS-Se on C57BL/6 mice was 136.89 mg/kg, and the LD<sub>50</sub> dose of TPS-Se was lesser than that of Na<sub>2</sub>SeO<sub>3</sub>. It can be seen that the toxicity of Inorganic Selenium form Na<sub>2</sub>SeO<sub>3</sub> is reduced by converting it into organic form TPS-Se.

#### 4 Conclusion

TPS-Se was prepared by the ascorbic acid-sodium selenite method and freeze-dried after dialysis in a 3500Da dialysis bag. The content of selenium in the product was 37.05%. An electron microscope was used to detect the changes in the morphology, and it was noticed that the changes were apparent. In combination with other characterization methods, it can be inferred that the sodium selenite is reduced to elemental selenium under the action of V<sub>C</sub> and elemental selenium is connected to TPS by C=O bond on TPS. Further, the antioxidant analysis showed that TPS-Se had advanced scavenging activity against DPPH free radical and ABTS free radical than TPS, indicating that TPS combined with selenium could significantly improve its antioxidant activity. This study provides a solid foundation for further research on TPS-Se.

#### Funding

This work was supported by Key Scientific Instrument Special Project of National Natural Science Foundation of China

(Project No. 81727805), Doctor start fund project (BK201803), Hubei Provincial Department of Education scientific Research Programme (B2019159), Hundred schools and hundred counties project (BXLBX0794, BXLBX0795), Xianning key special project for scientific and technological research and development (2021SFYF003).

## Acknowledgements

We thank Dr. Tao Chen ( Hubei University of Science and Technology) and Dr. Juntao Wang for assistance with the experiments and imaging.

## References

- Bai, X., & Bai, X. (2021). Antioxidant activity of a polysaccharide from *Dictyophora indusiata volva* and MECC analysis of its monosaccharide composition. *Journal of the Indian Chemical Society*, 98(10), 100146. <http://dx.doi.org/10.1016/j.jics.2021.100146>.
- Bakkaloglu, Z., Arici, M., & Karasu, S. (2021). Optimization of ultrasound-assisted extraction of turkish propolis and characterization of phenolic profile, antioxidant and antimicrobial activity. *Food Science and Technology*, 41(3), 687-695. <http://dx.doi.org/10.1590/fst.14520>.
- Cai, W., Hu, T., Bakry, A. M., Zheng, Z., Xiao, Y., & Huang, Q. (2018). Effect of ultrasound on size, morphology, stability and antioxidant activity of selenium nanoparticles dispersed by a hyperbranched polysaccharide from *Lignosus rhinocerotis*. *Ultrasonics Sonochemistry*, 42, 823-831. <http://dx.doi.org/10.1016/j.ultsonch.2017.12.022>. PMID:29429736.
- Huang, G., Mei, X., & Hu, J. (2017). The antioxidant activities of natural polysaccharides. *Current Drug Targets*, 18(11), 1296-1300. <http://dx.doi.org/10.2174/1389450118666170123145357>. PMID:28117001.
- Kaska, A., Deniz, N., Çiçek, M., & Mammadov, R. (2021). The screening of *Digitalis ferruginea* L. subsp. *ferruginea* for toxic capacities, phenolic constituents, antioxidant properties, mineral elements and proximate analysis. *Food Science and Technology*, 41(2), 505-512. <http://dx.doi.org/10.1590/fst.08620>.
- Ke, Q., Wang, S., Wang, Z., Zhou, H., Wang, C., Zheng, M. (2021). Effects of extraction temperature on polysaccharide content and biological activity of Qingzhuan dark tea. *Journal of Hubei University of Science and Technology*, 35(2), 93-97.
- Letavayová, L., Vlčková, V., & Brozmanová, J. (2006). Selenium: from cancer prevention to DNA damage. *Toxicology*, 227(1-2), 1-14. <http://dx.doi.org/10.1016/j.tox.2006.07.017>. PMID:16935405.
- Lew, S.-Y., Yow, Y.-Y., Lim, L.-W., & Wong, K.-H. (2020). Antioxidant-mediated protective role of *Herichium erinaceus* (Bull.: Fr.) Pers. Against oxidative damage in fibroblasts from Friedreich's ataxia patient. *Food Science and Technology*, 40(Suppl. 1), 264-272. <http://dx.doi.org/10.1590/fst.09919>.
- Li, F., Wang, F., Yu, F., Fang, Y., Xin, Z., Yang, F., Xu, J., Zhao, L., & Hu, Q. (2008). In vitro antioxidant and anticancer activities of ethanolic extract of selenium-enriched green tea. *Food Chemistry*, 111(1), 165-170. <http://dx.doi.org/10.1016/j.foodchem.2008.03.057>.
- Li, Q. (2018). Study on the activity of tea polysaccharide in puerh tea in lowering glucose and lipid. *Fujian Tea*, 40(6), 17.
- Liu, Y., Sun, Y., & Huang, G. (2018). Preparation and antioxidant activities of important traditional plant polysaccharides. *International Journal of Biological Macromolecules*, 111, 780-786. <http://dx.doi.org/10.1016/j.ijbiomac.2018.01.086>. PMID:29355627.
- Luo, Y., Zhang, C., Xu, C., Zuo, S., Liu, Y. (2012). Study on the extraction of polysaccharides from Alismataceae. *Journal of Tropical Agriculture Engineering*, 36(3), 5.
- Mao, Y. X. (2019). Study on anti-inflammatory immunity and anti-aging pharmacology of flavonoids. *Prescription Drugs in China*, 17(1), 39-40.
- Mei, X., Yi, C., & Huang, G. (2017). Preparation methods and antioxidant activities of polysaccharides and their derivatives. *Mini-Reviews in Medicinal Chemistry*, 17(10), 863-868. <http://dx.doi.org/10.2174/1389557517666170116114657>. PMID:28093971.
- Monobe, M., Ema, K., Kato, F., & Maeda-Yamamoto, M. (2008). Immunostimulating activity of a crude polysaccharide derived from green tea (*Camellia sinensis*) extract. *Journal of Agricultural and Food Chemistry*, 56(4), 1423-1427. <http://dx.doi.org/10.1021/jf073127h>. PMID:18232634.
- Pereira, I. M. C., Matos, J. D. No., Figueiredo, R. W., Carvalho, J. D. G., Figueiredo, E. A. T., Menezes, N. V. S., & Gaban, S. V. F. (2020). Physicochemical characterization, antioxidant activity, and sensory analysis of beers brewed with cashew peduncle (*Anacardium occidentale*) and orange peel (*Citrus sinensis*). *Food Science and Technology*, 40(3), 749-755. <http://dx.doi.org/10.1590/fst.17319>.
- Qing, M. (2013). *Pharmacology experimental tutorials*. Beijing: Science Press.
- Rayman, M. P. (2000). The importance of selenium to human health. *Lancet*, 356(9225), 233-241. [http://dx.doi.org/10.1016/S0140-6736\(00\)02490-9](http://dx.doi.org/10.1016/S0140-6736(00)02490-9). PMID:10963212.
- Ru, Y., Liu, K., Kong, X., Li, X., Shi, X., & Chen, H. (2020). Synthesis of selenylated polysaccharides from *Momordica charantia* L and its hypoglycemic activity in streptozotocin-induced diabetic mice. *International Journal of Biological Macromolecules*, 152, 295-304. <http://dx.doi.org/10.1016/j.ijbiomac.2020.02.288>. PMID:32112833.
- Souad, B., Brahim, L., Louiza, Z., et al (2021). In vitro comparative study on the antibacterial and the antioxidant activity of *Pergularia tomentosa* L. *Asian Journal of Research in Chemistry*, 14(4). <http://dx.doi.org/10.52711/0974-4150.2021.00049>.
- Ting, S., Chang, X., Hui, H., Wei, M., Bang, L., Xin, Y. (2019). Study on the inhibition of  $\alpha$ -glucosidase activity by crude polysaccharide of green brick tea. *Food Science and Technology*, 44(03), 194-199.
- Xia, C. T. (2019). Extraction and purification of tea polysaccharides and their biological activities. *Chemical Engineering Communications*, 45(5), 179.
- Yu, P. (2019). *Isolation purification and composition of neutral selenium polysaccharide from selenium-enriched sweet potato* (Dissertation). Liaoning University, Liaoning.
- Zheng, H.-G., Chen, J.-C., Weng, M.-J., Ahmad, I., & Zhou, C.-Q. (2020). Structural characterization and bioactivities of a polysaccharide from the stalk residue of *Pleurotus eryngii*. *Food Science and Technology*, 40(Suppl. 1), 235-241. <http://dx.doi.org/10.1590/fst.08619>.